Chapter 1

Finite Size and Isotope Shifts

"If we could only find a supply of atoms with 'point' nuclei we could measure ΔE and deduce R!"

K. S. Krane

1.1 Physical setup: what problem are we solving?

In solving the hydrogen atom one always assumes a point nucleus, $V = -Ze^2/(4\pi\varepsilon_0 r)$. Real nuclei are not points. Lectures 1–2 fixed the charge size from electron scattering: $R_0 \approx 1.2\,\mathrm{fm}\,A^{1/3}$ and a nearly universal skin $t \approx 2.3\,\mathrm{fm}$. The electron wave function penetrates to $r < R$, and inside the charge distribution the potential does *not* diverge as $1/r$. As a first approximation the nucleus may be taken as a uniformly charged sphere of radius R. Relative to a point nucleus, s-state energies then shift by an amount ΔE proportional to Z^4R^2 (derived below), which is precisely the finite-size correction introduced in Lecture 2.

No sample of point nuclei exists, so absolute finite-size shifts cannot be read off by simple subtraction. What can be measured cleanly is the difference between isotopes: same Z, different mass number and slightly different R. The isotope shift of K_α X-rays or optical lines then tests nuclear size, and in particular the $R \propto A^{1/3}$ law already suggested by electron scattering [6, 1]. Replacing the electron by a muon amplifies the same effect, because the muon Bohr orbit is about 207 times smaller.

1.2 Building the perturbation H_1 carefully

1.2.1 Point nucleus

For a hydrogen-like ion the electron (charge $-e$) in the field of a *point* nucleus (charge Ze) has potential energy

$$U_{\mathrm{point}}(r) = (-e)\cdot\left(\frac{1}{4\pi\varepsilon_0}\frac{Ze}{r}\right) = -\frac{Ze^2}{4\pi\varepsilon_0\, r}. \tag{1.1}$$

The minus sign means attraction: the energy is lowered when the electron approaches the nucleus. As $r \to 0$, $U_{\mathrm{point}} \to -\infty$. That infinite well is unphysical for a real nucleus of finite size.

1.2.2 Finite uniform sphere: field and potential

Assume a sphere of radius R with total charge Ze spread uniformly. Gauss's law gives the electric field $E(r)$ (radial, outward for $Z > 0$):

Outside ($r > R$). All charge is enclosed, so

$$E(r) = \frac{1}{4\pi\varepsilon_0}\frac{Ze}{r^2}, \qquad V(r) = \frac{1}{4\pi\varepsilon_0}\frac{Ze}{r} \quad (r > R), \tag{1.2}$$

exactly as for a point charge (with $V(\infty) = 0$).

Inside ($r \le R$). Only the charge fraction r^3/R^3 is enclosed:

$$E(r) = \frac{1}{4\pi\varepsilon_0}\frac{Ze\,r}{R^3}. \tag{1.3}$$

The electrostatic potential is continuous at $r = R$. Integrating inward from the surface,

$$\begin{aligned} V(r) &= V(R) + \int_r^R E(r')\,\mathrm{d}r' \\ &= \frac{1}{4\pi\varepsilon_0}\frac{Ze}{R} + \frac{1}{4\pi\varepsilon_0}\frac{Ze}{R^3}\int_r^R r'\,\mathrm{d}r' \\ &= \frac{1}{4\pi\varepsilon_0}\frac{Ze}{R} + \frac{1}{4\pi\varepsilon_0}\frac{Ze}{R^3}\cdot\frac{1}{2}(R^2 - r^2) \\ &= \frac{1}{4\pi\varepsilon_0}\frac{Ze}{2R}\left(3 - \frac{r^2}{R^2}\right). \end{aligned} \tag{1.4}$$

Check continuity at $r = R$

At $r = R$,

$$V(R) = \frac{1}{4\pi\varepsilon_0}\frac{Ze}{2R}(3 - 1) = \frac{1}{4\pi\varepsilon_0}\frac{Ze}{R},$$

which matches the exterior formula. At $r = 0$,

$$V(0) = \frac{1}{4\pi\varepsilon_0}\frac{3Ze}{2R},$$

finite (no singularity).

The electron potential energy is $U = -eV$:

$$U_{\text{finite}}(r) = \begin{cases} -\dfrac{Ze^2}{8\pi\varepsilon_0\,R}\left(3 - \dfrac{r^2}{R^2}\right), & r \le R, \\[2ex] -\dfrac{Ze^2}{4\pi\varepsilon_0\,r}, & r > R. \end{cases} \tag{1.5}$$

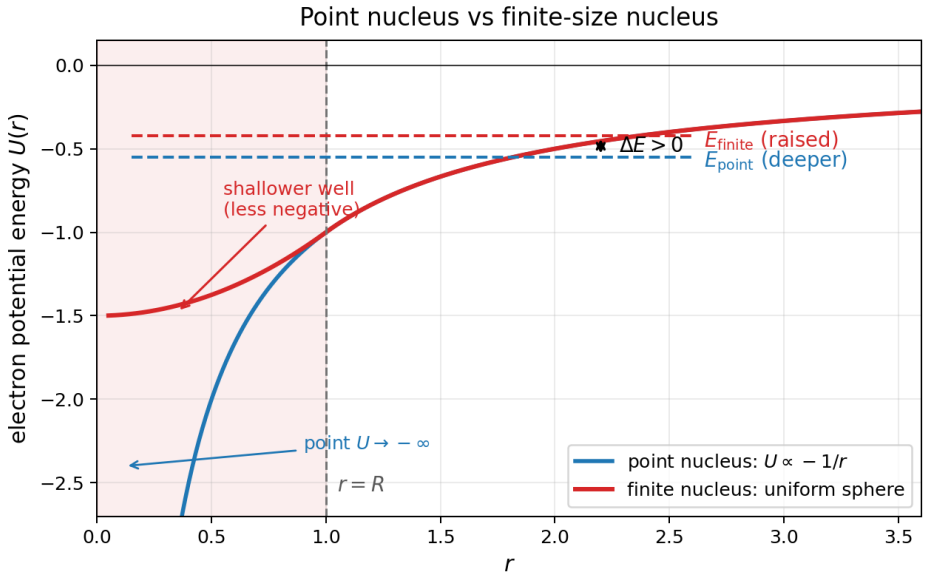

Figure 1.1: Electron potential energy for a point nucleus ($U \propto -1/r$, blue) and for a uniformly charged sphere of radius R (red). Outside the nucleus the two curves coincide. Inside, the finite-size well is shallower (less negative) because part of the nuclear charge lies outside the electron's position and attracts less strongly. The dashed lines are schematic $1s$ energies: raising the well raises the bound level from E_{point} to E_{finite} by $\Delta E > 0$ (weaker binding).

Remark

Compare U_{finite} and U_{point} at fixed $r < R$ in Figure 1.1. The finite-size well is *shallower* (less negative) because the electron, when inside the nucleus, does not feel the full Coulomb attraction of all the charge as if it were concentrated at a point. Raising the bottom of the well raises the **bound-state energy** of the electron, here the $1s$ energy E_{1s}. In the figure the dashed levels show this shift explicitly:

$$E_{\text{finite}} > E_{\text{point}} \qquad \text{(both negative; } |E_{\text{finite}}| < |E_{\text{point}}|\text{)},$$

so the finite-size correction is $\Delta E = E_{\text{finite}} - E_{\text{point}} > 0$.

Key idea

Reading Figure 1.1.

- At $r = 0$ the point potential dives to $-\infty$; the finite potential stays finite, $U(0) = -3Ze^2/(8\pi\varepsilon_0 R)$.
- For $0 < r < R$, red lies above blue: less attraction.
- For $r > R$, red = blue (all nuclear charge looks point-like).
- Bound-state energy E_{1s} (dashed) moves up with the well: weaker binding, $\Delta E > 0$.

1.2.3 Definition of the perturbation

Write the full Hamiltonian as $H = H_0 + H_1$, where H_0 is the usual point-nucleus hydrogen Hamiltonian and

$$H_1(r) \equiv U_{\text{finite}}(r) - U_{\text{point}}(r). \tag{1.6}$$

Outside the nucleus the two potentials agree, so $H_1 = 0$ for $r > R$. Inside,

$$\begin{aligned} H_1(r) &= -\frac{Ze^2}{8\pi\varepsilon_0 R}\left(3 - \frac{r^2}{R^2}\right) - \left(-\frac{Ze^2}{4\pi\varepsilon_0 r}\right) \\ &= -\frac{Ze^2}{8\pi\varepsilon_0 R}\left(3 - \frac{r^2}{R^2}\right) + \frac{Ze^2}{4\pi\varepsilon_0 r}. \end{aligned} \tag{1.7}$$

It is often convenient to factor $k \equiv Ze^2/(4\pi\varepsilon_0)$:

$$H_1(r) = k\left[\frac{1}{r} - \frac{3}{2R} + \frac{r^2}{2R^3}\right], \qquad r \le R. \tag{1.8}$$

Check $H_1(R) = 0$

At $r = R$,

$$\frac{1}{R} - \frac{3}{2R} + \frac{1}{2R} = \frac{2 - 3 + 1}{2R} = 0.$$

The perturbation vanishes smoothly at the nuclear surface. If a factor of two is dropped in the Coulomb term, this cancellation fails; that is a common algebraic trap.

Key idea

Only the interior region $r < R$ contributes to the energy shift. The entire calculation reduces to an integral of $H_1(r)$ weighted by the electron probability density inside the nucleus.

1.3 The $1s$ wave function, step by step

1.3.1 Normalised ground state

The hydrogen-like $1s$ wave function is

$$\psi_{1s}(r) = \frac{1}{\sqrt{\pi}}\left(\frac{Z}{a_0}\right)^{3/2} e^{-Zr/a_0}, \tag{1.9}$$

with

$$a_0 = \frac{4\pi\varepsilon_0\hbar^2}{m_e e^2} \approx 0.529\,\text{Å} = 5.29 \times 10^{-11}\,\text{m}. \tag{1.10}$$

Why these factors?

- The exponential e^{-Zr/a_0} is the solution of the radial Schrödinger equation for $n = 1$, $\ell = 0$. Larger Z pulls the cloud inward (effective Bohr radius a_0/Z).

- The prefactor is fixed by normalisation $\int |\psi|^2 \, \mathrm{d}^3 r = 1$. For a purely radial function, $\int_0^\infty 4\pi r^2 |\psi|^2 \, \mathrm{d}r = 1$.

Density at the origin. Set $r = 0$:

$$\psi_{1s}(0) = \frac{1}{\sqrt{\pi}} \left(\frac{Z}{a_0} \right)^{3/2}, \qquad |\psi_{1s}(0)|^2 = \frac{Z^3}{\pi a_0^3}. \tag{1.11}$$

The Z^3 dependence is crucial: heavier nuclei (larger Z) pack far more electron density near $r = 0$, so finite-size shifts grow rapidly with Z.

Caution

ψ_{1s} itself is proportional to $Z^{3/2}$, not Z^3. The quantity $Z^3/(\pi a_0^3)$ is $|\psi(0)|^2$, the probability density. Mixing the two is a frequent source of wrong powers of Z in ΔE.

1.3.2 First-order perturbation theory (what the formula means)

If the unperturbed eigenproblem is $H_0 \psi_n = E_n^{(0)} \psi_n$ and we add a small H_1, the first-order energy correction is

$$\Delta E_n = \langle \psi_n | H_1 | \psi_n \rangle = \int \psi_n^* \, H_1 \, \psi_n \, \mathrm{d}^3 r. \tag{1.12}$$

For the real $1s$ wave function this is simply the expectation value of H_1 in the unperturbed ground state:

$$\Delta E = \int |\psi_{1s}(r)|^2 H_1(r) \, \mathrm{d}^3 r. \tag{1.13}$$

Physical reading: average the extra potential energy H_1 with the probability density of finding the electron at each point. Since $H_1 = 0$ outside the nucleus, only the nuclear ball contributes.

1.4 Evaluating ΔE: full algebraic development

1.4.1 Write the integral in spherical coordinates

Because $|\psi_{1s}|^2$ and H_1 depend only on r,

$$\mathrm{d}^3 r = 4\pi r^2 \, \mathrm{d}r, \tag{1.14}$$

and

$$\Delta E = \int_0^R \underbrace{\frac{Z^3}{\pi a_0^3} e^{-2Zr/a_0}}_{|\psi_{1s}(r)|^2} H_1(r) \, 4\pi r^2 \, \mathrm{d}r. \tag{1.15}$$

(The factor e^{-2Zr/a_0} comes from $|e^{-Zr/a_0}|^2 = e^{-2Zr/a_0}$.)

1.4.2 Approximation: the exponential is almost 1

We must integrate only up to $r = R$. Compare length scales:

Quantity	Typical size	Comment
Nuclear radius R	$\sim 1 - -7\,\mathrm{fm}$	few fm
Bohr radius a_0	$5.29 \times 10^{-11}\,\mathrm{m}$	atomic scale
Ratio R/a_0	$\sim 2 \times 10^{-5}$	extremely small

For any $r \le R$,

$$\frac{2Zr}{a_0} \le \frac{2ZR}{a_0} \sim 2Z \times 10^{-5}. \tag{1.16}$$

Even for uranium ($Z = 92$),

$$\frac{2ZR}{a_0} \approx 1.8 \times 10^{-3} \ll 1. \tag{1.17}$$

Taylor expand:

$$e^{-2Zr/a_0} = 1 - \frac{2Zr}{a_0} + \cdots \approx 1, \tag{1.18}$$

with a relative error of order 10^{-3} or less for electronic atoms. Therefore, to an excellent approximation,

$$\Delta E \approx |\psi_{1s}(0)|^2 \int_0^R H_1(r)\, 4\pi r^2\, \mathrm{d}r = |\psi_{1s}(0)|^2 \int_{r<R} H_1\, \mathrm{d}^3 r. \tag{1.19}$$

Key idea

Because the nucleus is a speck on the atomic scale, the electron density hardly varies across it. Pull $|\psi(0)|^2$ out of the integral; only the volume integral of H_1 remains.

1.4.3 Volume integral of H_1 (line by line)

Start from Equation (1.8):

$$H_1(r) = k\left(\frac{1}{r} - \frac{3}{2R} + \frac{r^2}{2R^3}\right), \qquad k = \frac{Ze^2}{4\pi\varepsilon_0}. \tag{1.20}$$

Then

$$\begin{aligned} I &\equiv \int_{r<R} H_1\, \mathrm{d}^3 r = \int_0^R H_1(r)\, 4\pi r^2\, \mathrm{d}r \\ &= 4\pi k \int_0^R \left(r - \frac{3r^2}{2R} + \frac{r^4}{2R^3}\right) \mathrm{d}r. \end{aligned} \tag{1.21}$$

Integrate term by term:

$$\int_0^R r\, \mathrm{d}r = \frac{R^2}{2}, \tag{1.22}$$

$$\int_0^R \frac{3r^2}{2R}\, \mathrm{d}r = \frac{3}{2R} \cdot \frac{R^3}{3} = \frac{R^2}{2}, \tag{1.23}$$

$$\int_0^R \frac{r^4}{2R^3}\, \mathrm{d}r = \frac{1}{2R^3} \cdot \frac{R^5}{5} = \frac{R^2}{10}. \tag{1.24}$$

The first two contributions cancel:

$$\frac{R^2}{2} - \frac{R^2}{2} + \frac{R^2}{10} = \frac{R^2}{10}. \tag{1.25}$$

Therefore

$$I = 4\pi k \cdot \frac{R^2}{10} = \frac{2\pi}{5}\, k\, R^2 = \frac{2\pi}{5}\frac{Ze^2}{4\pi\varepsilon_0} R^2 = \frac{Ze^2 R^2}{10\,\varepsilon_0}. \tag{1.26}$$

Why the cancellation?

The $1/r$ and constant pieces of H_1 rearrange the Coulomb singularity into a finite well. Their weighted integrals over the ball cancel, leaving only the r^2 piece of the interior potential, which produces the factor $R^2/10$. That is why $\Delta E \propto R^2$, not R^3: after cancellation one power of R is lost relative to a naive volume estimate.

1.4.4 Assemble ΔE

$$\begin{aligned}\Delta E &= |\psi_{1s}(0)|^2\, I = \frac{Z^3}{\pi a_0^3} \cdot \frac{2\pi}{5} \cdot \frac{Ze^2}{4\pi\varepsilon_0} R^2 \\ &= \frac{Z^3}{\pi a_0^3} \cdot \frac{Ze^2 R^2}{10\,\varepsilon_0} \cdot \frac{2\pi}{2\pi} \\ &= \frac{Z^4 e^2 R^2}{10\pi\,\varepsilon_0\, a_0^3}.\end{aligned} \tag{1.27}$$

Final formula: $1s$ finite-size shift (uniform sphere)

$$\boxed{\Delta E_{1s} = \frac{Z^4 e^2 R^2}{10\pi\,\varepsilon_0\, a_0^3} > 0}$$

How to read the powers.

- $Z^4 = Z \cdot Z^3$: one Z from the Coulomb strength Ze^2, and Z^3 from $|\psi(0)|^2$.
- R^2: residual after the integral cancellation discussed above.
- $1/a_0^3$: denser electron cloud for smaller Bohr radius.
- Positive sign: the well is shallower, so the level moves *up* (less bound).

Example: scaling with Z and R

Compare hydrogen ($Z = 1$, $R \sim 1\,\text{fm}$) with mercury ($Z = 80$, $R \sim 7\,\text{fm}$):

$$\frac{\Delta E(\text{Hg})}{\Delta E(\text{H})} \sim 80^4 \times 7^2 \approx 4.1 \times 10^7 \times 49 \approx 2 \times 10^9.$$

Hydrogen's shift is $\sim 10^{-10}$ of $|E_{1s}|$; mercury's absolute shift is still only $\sim 0.1\,\text{eV}$, but that is measurable against a K_α energy of $\sim 100\,\text{keV}$.

1.4.5 Link to the mean-square radius

For a general spherical charge density (not necessarily uniform), the leading finite-size shift is obtained by expanding the Coulomb kernel for a localised charge and retaining the first correction beyond the monopole. With the electron density nearly constant across the nucleus,

$$\begin{aligned}\Delta E_{1s} &= |\psi_{1s}(0)|^2 \int [U_{\text{finite}}(\boldsymbol{r}) - U_{\text{point}}(\boldsymbol{r})]\,\mathrm{d}^3 r \\ &= \frac{2\pi}{3}\frac{Ze^2}{4\pi\varepsilon_0}\langle r^2\rangle_{\text{ch}}|\psi_{1s}(0)|^2,\end{aligned} \tag{1.28}$$

where the second line follows after one angular average and one radial partial integration (the same identity used in Lecture 2). For a uniform sphere,

$$\langle r^2\rangle = \frac{\int_0^R r^2 \cdot 4\pi r^2\,\mathrm{d}r}{\frac{4}{3}\pi R^3} = \frac{3}{5}R^2. \tag{1.29}$$

Inserting this into Equation (1.28) recovers Equation (1.27):

$$\frac{2\pi}{3}\,k\cdot\frac{3}{5}R^2\cdot\frac{Z^3}{\pi a_0^3} = \frac{2\pi}{5}\,kR^2\cdot\frac{Z^3}{\pi a_0^3} = \frac{Z^4e^2R^2}{10\pi\varepsilon_0 a_0^3}. \tag{1.30}$$

So the uniform-sphere calculation is a special case of a more general theorem: the leading shift measures $\langle r^2\rangle_{\text{ch}}$.

Writing E_{1s}^{point} for the unperturbed energy,

$$E_{1s} = E_{1s}^{\text{point}} + \Delta E_{1s}. \tag{1.31}$$

1.5 K_α X-rays: from levels to a measurable line

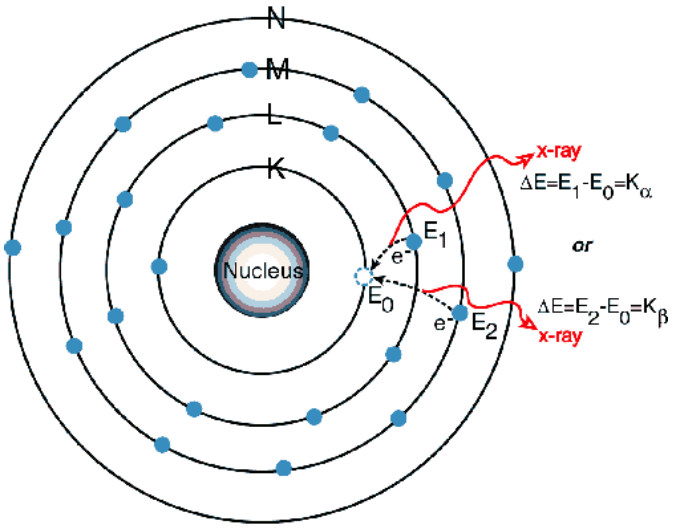

Figure 1.2: Atomic shells. A vacancy in the K shell ($1s$) is filled from a higher shell, emitting an X-ray. K_α corresponds mainly to $2p \to 1s$; K_β involves higher initial levels.

1.5.1 What is measured?

If a $1s$ electron is removed, an electron from a higher shell can drop into the vacancy. The energy difference is emitted as a characteristic X-ray (Figure 1.2). The K_α complex is dominated by $2p \to 1s$ transitions.

Historical note: Henry Moseley (1887–1915)

Henry Gwyn Jeffreys Moseley showed (1913–1914) that characteristic X-ray frequencies scale as $(Z-1)^2$, establishing Z as the true ordering parameter of the elements. That is why K_α energies are such a clean probe of nuclear charge and, through isotope shifts, of nuclear size.

1.5.2 Point-nucleus level energies

For a hydrogen-like ion,

$$E_n^{\text{point}} = -\frac{m_e Z^2 e^4}{8\varepsilon_0^2 h^2 n^2} = -\frac{Z^2}{n^2}\,\text{Ry}, \qquad \text{Ry} \approx 13.6\,\text{eV}. \tag{1.32}$$

Thus

$$E_{1s}^{\text{point}} = -Z^2\,\text{Ry}, \qquad E_2^{\text{point}} = -\frac{Z^2}{4}\,\text{Ry} \quad (\text{includes } 2p). \tag{1.33}$$

Photon energy for $2p \to 1s$. The electron falls from a less-bound level to a more-bound level. The photon energy is

$$\begin{aligned} E_{K_\alpha}^{\text{point}} &= E_2^{\text{point}} - E_{1s}^{\text{point}} \\ &= \left(-\frac{Z^2}{4} + Z^2\right)\text{Ry} = \frac{3}{4}\,Z^2\,\text{Ry}. \end{aligned} \tag{1.34}$$

(For real atoms, screening replaces Z by $\approx Z-1$, as in Moseley's law; the structure of the finite-size argument is unchanged.)

1.5.3 How ΔE_{1s} changes K_α

In non-relativistic theory, p-state wave functions vanish at $r = 0$, so their finite-size shifts are much smaller than that of $1s$. Keeping only ΔE_{1s},

$$\begin{aligned} E_{K_\alpha} &= E_2^{\text{point}} - (E_{1s}^{\text{point}} + \Delta E_{1s}) \\ &= (E_2^{\text{point}} - E_{1s}^{\text{point}}) - \Delta E_{1s} \\ &= E_{K_\alpha}^{\text{point}} - \Delta E_{1s}. \end{aligned} \tag{1.35}$$

Sign: why K_α softens

- Finite size raises E_{1s} (makes it less negative).
- E_2 is almost unchanged.
- The gap $E_2 - E_{1s}$ therefore shrinks.

- The emitted X-ray has slightly lower energy.

Key idea

$$E_{K_\alpha} = E_{K_\alpha}^{\text{point}} - \frac{Z^4 e^2 R^2}{10\pi\,\varepsilon_0\, a_0^3}.$$

Larger $R \Rightarrow$ smaller E_{K_α}.

1.6 Isotope shifts: cancelling everything except R

1.6.1 Why isotopes?

Two isotopes of the same element have:

- the *same* Z (same Coulomb strength, same electronic structure to an excellent approximation);
- *different* A, hence different nuclear radii $R(A)$.

All point-nucleus pieces of E_{K_α} cancel in a difference, and only the finite-size terms survive.

1.6.2 Algebra for two isotopes

Let the reference isotope have mass number A_0 and radius R_0, and another isotope have A and R. Then

$$E_{K_\alpha}(A_0) = E_{K_\alpha}^{\text{point}} - CR_0^2, \tag{1.36}$$
$$E_{K_\alpha}(A) = E_{K_\alpha}^{\text{point}} - CR^2, \tag{1.37}$$

where we abbreviated the positive constant

$$C \equiv \frac{Z^4 e^2}{10\pi\,\varepsilon_0\, a_0^3}. \tag{1.38}$$

Subtract:

$$\begin{aligned}\Delta E_{K_\alpha} &\equiv E_{K_\alpha}(A) - E_{K_\alpha}(A_0)\\ &= (E_{K_\alpha}^{\text{point}} - CR^2) - (E_{K_\alpha}^{\text{point}} - CR_0^2)\\ &= C(R_0^2 - R^2).\end{aligned} \tag{1.39}$$

Interpretation. If the second isotope is heavier, typically $R > R_0$, so $R_0^2 - R^2 < 0$ and $\Delta E_{K_\alpha} < 0$. The heavier isotope's K_α line lies at slightly lower energy. Experimental plots often display $-\Delta E_{K_\alpha}$ (a positive quantity that grows with A).

1.6.3 Insert $R_0 = 1.2\,\text{fm}\,A^{1/3}$

Electron-scattering systematics give the half-density radius [1]

$$R = R_0 = 1.2\,\text{fm} \times A^{1/3} \quad \Rightarrow \quad R^2 = (1.2\,\text{fm})^2\, A^{2/3}. \tag{1.40}$$

Then

$$\Delta E_{K_\alpha} = C\,(1.2\,\mathrm{fm})^2(A_0^{2/3} - A^{2/3}) = \frac{Z^4 e^2}{10\pi\,\varepsilon_0\,a_0^3}(1.2\,\mathrm{fm})^2(A_0^{2/3} - A^{2/3}). \tag{1.41}$$

Equivalently,

$$-\Delta E_{K_\alpha} = C\,(1.2\,\mathrm{fm})^2(A^{2/3} - A_0^{2/3}). \tag{1.42}$$

What to plot

Fix a reference isotope A_0. For each other isotope A, compute $-\Delta E_{K_\alpha}$ and plot it against $A^{2/3}$.

- **If the points fall on a straight line**, the data support $R \propto A^{1/3}$.
- **The slope** equals $C \times (1.2\,\mathrm{fm})^2$ if the R_0 law holds; a measured slope is a consistency check on that same coefficient.

Takeaway

Experimental checklist:

1. Measure E_{K_α} for several isotopes of one element.
2. Form shifts relative to a reference isotope.
3. Plot $-\Delta E$ versus $A^{2/3}$.
4. Linearity $\Rightarrow R \propto A^{1/3}$; slope checks $R_0 = 1.2\,\mathrm{fm}\,A^{1/3}$ from form-factor data [1].

1.6.4 Mercury data

Mercury ($Z = 80$) has several stable isotopes near $A \sim 200$. Figure 1.3 plots $-\Delta E$ against $A^{2/3}$ with ^{198}Hg as reference. The near-linearity is the experimental signature of $R \propto A^{1/3}$. Small odd–even staggering reflects pairing and slight deformation beyond the ideal spherical model.

Example: how small is the shift?

For mercury,

$$E_{K_\alpha} \sim 100\,\mathrm{keV} = 10^5\,\mathrm{eV}, \qquad |\Delta E| \sim 0.1\,\mathrm{eV} \text{ between nearby isotopes.}$$

The fractional change is

$$\frac{|\Delta E|}{E_{K_\alpha}} \sim 10^{-6}.$$

That is one part per million: tiny, but accessible to modern precision X-ray spectroscopy. The slope of the line, together with many other experiments, gives the standard $r_0 \approx 1.2\,\mathrm{fm}$.

1.7 Muonic atoms: the same maths with a heavy lepton

Electronic shifts are parts per million. Nature provides a louder version of the same calculation: replace the electron by a muon.

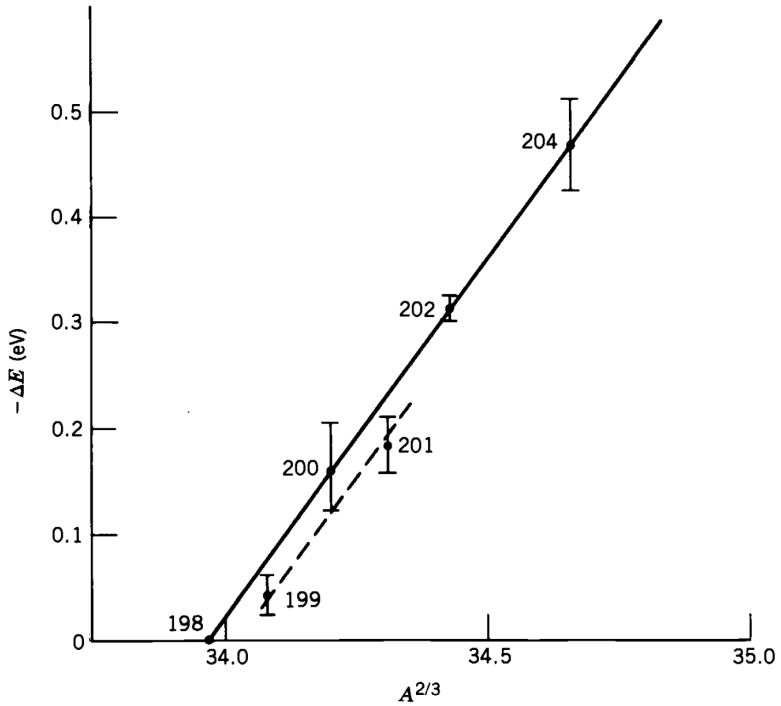

Figure 1.3: K_α isotope shifts in mercury ($Z = 80$), plotted as $-\Delta E$ versus $A^{2/3}$ relative to ^{198}Hg. Even and odd isotopes lie on nearly straight lines, as expected if $R \propto A^{1/3}$. After standard isotope-shift data, *Introductory Nuclear Physics*.

1.7.1 Muon basics

The muon μ^- has charge $-e$ and mass

$$m_\mu \approx 207\, m_e. \tag{1.43}$$

Lifetime $\tau_\mu \approx 2.2\,\mu\text{s}$ (rest frame), long enough to be captured into atomic orbits and emit X-rays before decaying ($\mu^- \to e^- \bar{\nu}_e \nu_\mu$).

Historical note: Carl D. Anderson (1905–1991)

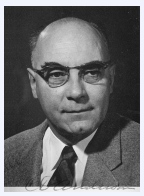

Carl David Anderson discovered the positron (1932) and the muon in cosmic rays (1936, with Neddermeyer). The muon was first mistaken for Yukawa's meson; it is in fact a heavy lepton. Anderson's particle is the probe behind modern muonic-atom determinations of nuclear charge radii.

1.7.2 How the Bohr radius scales

The Bohr radius comes from balancing Coulomb attraction against kinetic energy. With reduced mass μ of the orbiting lepton and the nucleus,

$$a_\mu = \frac{4\pi\varepsilon_0\,\hbar^2}{\mu e^2} = a_{\mathrm{B}}\,\frac{m_e}{\mu}. \tag{1.44}$$

For an electron on a heavy nucleus, $\mu \approx m_e$ and $a \approx a_{\mathrm{B}}$. For a muon, $\mu \approx m_\mu$ (still $\ll m_{\mathrm{nucleus}}$), so

$$a_\mu = a_0 \frac{m_e}{m_\mu} \approx \frac{a_0}{207}. \tag{1.45}$$

Caution

The mass ratio is ≈ 207, not 27. Hence $a_\mu = a_0/207$. Using 27 underestimates how tightly the muon is bound by almost an order of magnitude in linear size.

1.7.3 How ΔE scales for a muon

Repeat Equation (1.27) with $a_0 \to a_\mu$ and $m_e \to m_\mu$ in the wave function. The structure is unchanged:

$$\Delta E^{(\mu)} = \frac{Z^4 e^2 R^2}{10\pi\,\varepsilon_0\, a_\mu^3}. \tag{1.46}$$

Compared with the electronic shift,

$$\frac{\Delta E^{(\mu)}}{\Delta E^{(e)}} = \left(\frac{a_0}{a_\mu}\right)^3 = \left(\frac{m_\mu}{m_e}\right)^3 \approx 207^3 \approx 8.9 \times 10^6. \tag{1.47}$$

So muonic finite-size shifts are roughly *ten million times* larger in the naive scaling (before accounting for the fact that for heavy nuclei the muon orbit is so small that the constant-ψ approximation and non-relativistic theory both need upgrading).

Example: muon K-shell size in lead

Electron K radius $\sim a_0/Z$. Muon K radius $\sim a_\mu/Z = a_0/(207\,Z)$. For lead ($Z = 82$),

$$\frac{a_\mu}{Z} \approx \frac{0.529\,\text{Å}}{207 \times 82} \approx 3\,\text{fm},$$

comparable to the nuclear radius. The muon wave function overlaps the nuclear charge distribution strongly; precision $\langle r^2 \rangle$ follows from measured muonic X-ray energies.

Key idea

Same formulae, different mass: muonic atoms turn a parts-per-million electronic effect into a large, accurately measurable shift, at the price of a more careful (often relativistic, numerical) treatment for heavy Z.

Remark

For heavy nuclei one no longer pulls $|\psi(0)|^2$ out as a constant: the muon $1s$ state varies over nuclear dimensions. One then solves the Dirac equation in the electrostatic potential of a realistic $\rho(r)$ and adjusts $\langle r^2 \rangle$ (or a full density model) to match the observed transitions. The conceptual origin of the shift is still the same H_1 we built in Section 1.2.

1.8 Worked summary of the mathematics

One-page derivation map

1. $U_{\text{point}} = -\dfrac{Ze^2}{4\pi\varepsilon_0 r}$.
2. Uniform sphere $\Rightarrow U_{\text{finite}} = -\dfrac{Ze^2}{8\pi\varepsilon_0 R}(3 - r^2/R^2)$ for $r \le R$.
3. $H_1 = U_{\text{finite}} - U_{\text{point}}$ (zero outside).
4. $\Delta E = \int |\psi_{1s}|^2 H_1 \, \mathrm{d}^3 r$.
5. $e^{-2Zr/a_0} \approx 1$ on $r \le R$ because $R \ll a_0$.
6. $\Delta E \approx |\psi(0)|^2 \int H_1 \, \mathrm{d}^3 r$.
7. $\int H_1 \, \mathrm{d}^3 r = \dfrac{2\pi}{5} k R^2$ after cancellation of two terms in the radial integral.
8. $|\psi(0)|^2 = Z^3/(\pi a_0^3) \Rightarrow \Delta E = \dfrac{Z^4 e^2 R^2}{10\pi\varepsilon_0 a_0^3}$.
9. $E_{K_\alpha} = E_{K_\alpha}^{\text{point}} - \Delta E$.
10. Isotope difference $\propto (R_0^2 - R^2)$; with $R = 1.2\,\text{fm}\, A^{1/3}$, plot vs $A^{2/3}$.
11. Muon: replace $a_0 \to a_0/207$; shift grows as 207^3.

1.9 Three experimental routes to nuclear size

1. **Electron scattering** (Lectures 1–2). Maps $F(q)$ and $\rho_p(r)$; yields $R_0 = 1.2\,\text{fm}\, A^{1/3}$ and $a = 0.52\,\text{fm} \pm 0.01\,\text{fm}$ [1].
2. **Electronic K_α isotope shifts** (this lecture). $\Delta E_{1s} = Z^4 e^2 R^2/(10\pi\varepsilon_0 a_0^3)$ softens K_α; differences test $A^{1/3}$ via linearity in $A^{2/3}$.
3. **Muonic atoms**. Same maths with $a_\mu = a_0/207$; much larger shifts and precise $\langle r^2 \rangle_{\text{ch}}$.

Takeaway

The algebra is lengthy, but the physics is simple: a finite nucleus softens the Coulomb singularity, raises s-state energies by an amount $\propto Z^4 R^2$, and that shift is visible in X-rays once you compare isotopes or switch to muons. The same $R_0 = 1.2\,\text{fm}\, A^{1/3}$ that appears in electron scattering [1] reappears in the slope of the isotope-shift plot.

Next. Lecture 4 leaves size for *energy*: binding energy, the B/A curve, and the liquid-drop SEMF. Lecture 5 then turns the same mass formula into mass parabolas and β stability.

1.10 Deeper physics: comparing size probes

Lectures 1–3 measure nuclear size three ways. The results agree at the percent level only when each method quotes a carefully defined moment of ρ_{ch} [6, 1, 2].

1.10.1 Electron scattering vs atomic shifts

Probe	What is measured	Sensitivity
Elastic e^- scattering	$\lvert F(q)\rvert^2 \to \rho_{\mathrm{ch}}(r)$	Full radial profile; model-dependent at large q
Electronic K_α / optical isotope shift	$\Delta\langle r^2\rangle$ between isotopes	Relative radii; absolute scale needs calibration
Muonic atoms	Large finite-size shift $\propto m_\mu^3$	Absolute $\langle r^2\rangle_{\mathrm{ch}}$ for many Z

Muonic $1s$ levels are far more sensitive than electronic ones because the Bohr radius scales as $1/m$: $m_\mu/m_e \approx 207$ compresses the orbit by the same factor and boosts the overlap with the nucleus by $\sim 207^3$. That is why muonic X-rays became a precision tool for charge radii once muon beams were available [2, 6].

1.10.2 Mean-square radius as the universal intermediate

All three methods ultimately quote moments of ρ_{ch}. For a uniform sphere of radius R,

$$\langle r^2\rangle = \tfrac{3}{5}R^2, \tag{1.48}$$

so $R_{\mathrm{eq}} = \sqrt{5/3}\,\langle r^2\rangle^{1/2}$. Isotope-shift formulae depend on $\delta\langle r^2\rangle$, not on a model-dependent surface thickness. Electron scattering at low q measures the same $\langle r^2\rangle$ from the form-factor curvature (Lecture 1). Agreement among methods is a major empirical success of nuclear charge-density physics.

Order of magnitude for the $1s$ shift

For $Z \sim 80$ and $R \sim 7\,\mathrm{fm}$, the electronic finite-size correction to the $1s$ level is only of order eV–keV on a keV–MeV scale, yet modern X-ray and laser spectroscopy resolve isotope differences cleanly. The same algebra with $m \to m_\mu$ yields keV to MeV shifts: muonic spectroscopy is a nuclear, not atomic, measurement in disguise [6].

Key idea

Absolute shift vs isotope difference. The absolute finite-size correction $\Delta E(A, Z)$ is entangled with atomic-structure uncertainties. Differences $\Delta E(A, Z) - \Delta E(A', Z)$ cancel most of that background and isolate $\delta\langle r^2\rangle$. Electron scattering and muonic atoms calibrate the absolute scale that isotope shifts then track along a chain.

1.11 Further physics: separation energies and the isotope-shift ladder

Atomic size enters spectroscopy through level shifts; nuclear size also leaves fingerprints in the energies needed to remove a nucleon. The neutron and proton separation energies

$$S_n = [M(A-1,Z)+m_n-M(A,Z)]c^2, \qquad S_p = [M(A-1,Z-1)+m(^1\mathrm{H})-M(A,Z)]c^2 \quad (1.49)$$

are the nuclear analogues of ionisation energies: they probe valence nucleons. Sharp jumps in S_n or S_p at closed shells are shell signatures; smooth trends with A and Z follow the SEMF surface, Coulomb, and pairing terms (Lectures 4–5) [13, 6, 1].

Finite-size shifts of s levels and separation-energy systematics are complementary: both are sensitive to how tightly the outer nucleons (or the electron cloud near $r = 0$) feel the nuclear interior.

1.11.1 Mirror nuclei and a Coulomb-radius estimate

Binding-energy differences of mirror pairs provide an independent size check. For example,

$$B(^3\mathrm{H}) - B(^3\mathrm{He}) \approx 0.76\,\mathrm{MeV}$$

is largely the Coulomb energy of the two protons in ^{3}He. Writing

$$\Delta B \approx \frac{e^2}{4\pi\varepsilon_0}\left\langle\frac{1}{r_{12}}\right\rangle \sim \frac{e^2}{4\pi\varepsilon_0 R}$$

yields $R \sim 2\,\mathrm{fm}$, consistent with other light-nucleus radii [14]. Finite-size isotope shifts (this lecture) and mirror Coulomb differences are two faces of the same electrostatic physics.

1.11.2 Isotope-shift ladder: optical, K_α, and muonic

Three experimental ladders measure the same change of nuclear mean-square radius between isotopes A and A' [6, 1]:

1. **Optical isotope shifts** (valence transitions). The electron density at the nucleus is small, so shifts are tiny (parts in 10^6 of optical frequencies) but laser spectroscopy resolves them for long chains of radioactive isotopes.

2. K_α **X-ray isotope shifts.** The $2p \to 1s$ transition energy difference between isotopes is essentially the difference of $1s$ finite-size shifts, because p wave functions vanish at $r = 0$. A plot of ΔE_K versus $A^{2/3}$ is approximately linear for a sequence of isotopes [6].

3. **Muonic X rays.** The muon Bohr radius is $\sim m_e/m_\mu$ times smaller than the electronic one, so the muon spends a much larger fraction of its time inside the nucleus. Isotope shifts are correspondingly huge and dominate over many atomic-structure uncertainties.

For a uniform sphere the first-order $1s$ finite-size shift scales as

$$\Delta E_{1s} \propto Z^4\,R^2\,|\psi_{1s}(0)|^2, \quad (1.50)$$

so $\Delta E(A) - \Delta E(A') \propto R^2(A) - R^2(A')$. All three methods, after careful atomic-structure corrections, return R_0 consistent with electron scattering ($\sim 1.2\,\mathrm{fm}$).

1.11.3 Forward look: magic numbers in separation energies

Just as atomic ionisation energies jump at noble-gas Z, nuclear separation energies jump at magic N or Z:

$$N, Z = 2, 8, 20, 28, 50, 82, 126. \tag{1.51}$$

Lead isotopes show a clear discontinuity in S_n at $N = 126$ (^{208}Pb). The SEMF alone is smooth; the excess binding of magic and doubly magic nuclei relative to the liquid-drop fit is a shell-model signature that returns when single-particle potentials are discussed [14, 6]. For now it is enough that size probes and separation energies both organise the chart of nuclides before binding-energy systematics take over in Lecture 4.

1.12 Problems with solutions

Problem 3.1 — Finite-size shift for a uniform sphere

Show that for a hydrogen-like $1s$ electron and a uniform nuclear charge of radius $R \ll a_0/Z$, the first-order energy shift relative to a point nucleus is

$$\Delta E \approx \frac{2}{5}\frac{Z^4 e^2}{4\pi\varepsilon_0}\frac{R^2}{a_0^3}$$

(up to the standard hydrogenic normalisation constants; cf. Krane §3.1). Estimate ΔE for $Z = 80$, $R = 7\,\mathrm{fm}$.

Solution 3.1

Inside a uniform sphere the potential energy of an electron is

$$U_{\mathrm{finite}}(r) = -\frac{Ze^2}{8\pi\varepsilon_0 R}\left(3 - \frac{r^2}{R^2}\right), \qquad r \le R,$$

while $U_{\mathrm{point}} = -Ze^2/(4\pi\varepsilon_0 r)$. Their difference H_1 vanishes for $r > R$. With $|\psi_{1s}(0)|^2 = Z^3/(\pi a_0^3)$ nearly constant over the nucleus,

$$\int_{r<R} H_1\,\mathrm{d}^3r = \frac{2\pi}{5}\frac{Ze^2}{4\pi\varepsilon_0}R^2,$$

$$\Delta E = |\psi(0)|^2 \int H_1\,\mathrm{d}^3r = \frac{2}{5}\frac{Z^4e^2}{4\pi\varepsilon_0}\frac{R^2}{a_0^3}.$$

(The factor 2/5 is the uniform-sphere special case of the $\langle r^2\rangle = \frac{3}{5}R^2$ theorem.) For $Z = 80$, $R = 7\,\mathrm{fm} = 7\times10^{-15}\,\mathrm{m}$, $a_0 = 5.29\times10^{-11}\,\mathrm{m}$,

$$\frac{R^2}{a_0^3} \sim 4\times10^{-23}\,\mathrm{m}^{-1}, \qquad \Delta E \sim \text{eV–tens of eV}$$

on a K-shell scale of tens of keV: a small but measurable isotope-shift effect for electronic X rays, and a large effect for muons.

Problem 3.2 — Isotope shift and $A^{1/3}$

Two isotopes of the same element have mass numbers A and A' and radii $R = r_0 A^{1/3}$, $R' = r_0 (A')^{1/3}$. Argue that the difference of finite-size $1s$ shifts scales as

$$\Delta E(A) - \Delta E(A') \propto Z^4 (A^{2/3} - A'^{2/3}).$$

Why is a plot of K_α X-ray isotope shifts versus $A^{2/3}$ expected to be approximately linear?

Solution 3.2

From Problem 3.1, $\Delta E \propto Z^4 R^2$ and $R^2 \propto A^{2/3}$. Hence

$$\delta(\Delta E) \propto Z^4 (A^{2/3} - A'^{2/3}).$$

Plotting measured isotope shifts against $A^{2/3}$ (relative to a reference isotope) should be nearly linear with slope fixed by r_0. Deviations encode shell effects and deformation [6].

Problem 3.3 — Muonic enhancement

By what factor does the finite-size shift grow if the electron is replaced by a muon ($m_\mu / m_e \approx 207$), all else equal?

Solution 3.3

The Bohr radius scales as $1/\mu$, and $|\psi(0)|^2 \propto 1/a^3 \propto \mu^3$. Replacing m_e by m_μ therefore multiplies ΔE by

$$\Delta E_\mu = \left(\frac{m_\mu}{m_e} \right)^3 \Delta E_e \approx 207^3 \Delta E_e = 8.86 \times 10^6 \, \Delta E_e \sim 9 \times 10^6 \, \Delta E_e.$$

Caveat: for heavy nuclei the muon $1s$ orbit has size comparable to R, so the constant-$\psi(0)$ approximation and non-relativistic theory both need upgrading; the factor $\sim 10^7$ is the scaling estimate, not a precision prediction. Muonic K_α X-rays are a nuclear-size measurement, not an atomic one.

Bibliography

[1] R. A. Dunlap, *An Introduction to the Physics of Nuclei and Particles* (2nd ed.), IOP Publishing, Bristol (2023), DOI: 10.1088/978-0-7503-6094-4, Ch. 3 (Nuclear composition and size).

[2] W. Demtröder, *Nuclear and Particle Physics*, Undergraduate Lecture Notes in Physics, Springer, Cham (2023).

[3] S. Petrera, *Problems and Solutions in Nuclear and Particle Physics*, UNITEXT for Physics, Springer, Cham (2019).

[4] F. Terranova, *A Modern Primer in Particle and Nuclear Physics*, Oxford University Press (2021).

[5] S. D'Auria, *Introduction to Nuclear and Particle Physics*, Undergraduate Lecture Notes in Physics, Springer, Cham (2018).

[6] K. S. Krane, *Introductory Nuclear Physics*, Wiley, New York (1988).

[7] R. Hofstadter, "Electron scattering and nuclear structure," Rev. Mod. Phys. **28**, 214 (1956).

[8] H. F. Ehrenberg, R. Hofstadter, U. Meyer-Berkhout, D. G. Ravenhall, and S. E. Sobottka, "High-Energy Electron Scattering and the Charge Distribution of Carbon-12 and Oxygen-16," Phys. Rev. **113**, 666 (1959).

[9] H. Yukawa, "On the interaction of elementary particles. I," Proc. Phys.-Math. Soc. Japan **17**, 48 (1935).

[10] R. D. Woods and D. S. Saxon, "Diffuse surface optical model for nucleon-nuclei scattering," Phys. Rev. **95**, 577 (1954).

[11] H. G. J. Moseley, "The high-frequency spectra of the elements," Phil. Mag. **26**, 1024 (1913); **27**, 703 (1914).

[12] C. F. von Weizsäcker, "Zur Theorie der Kernmassen," Z. Phys. **96**, 431 (1935).

[13] P. Cappellaro, *Introduction to Applied Nuclear Physics* (MIT OpenCourseWare / LibreTexts), CC BY-NC-SA 4.0.

[14] J.-L. Basdevant, J. Rich, and M. Spiro, *Fundamentals in Nuclear Physics: From Nuclear Structure to Cosmology*, Springer, New York (2005).

[15] D. Tong, *Particle Physics*, Lecture notes (University of Cambridge / CERN school notes).